Closure approximations for the Doi theory: Which to use in simulating complex flows of liquid-crystalline polymers?

J. Feng, C. V. Chaubal, and L. G. Leal[a)]

Department of Chemical Engineering, University of California, Santa Barbara, California 93106-5080

(Received 17 December 1997; final revision received 15 June 1998)

Synopsis

The goal of this article is to determine which closure model should be used in simulating complex flows of liquid-crystalline polymers (LCPs). We examine the performance of six closure models: the quadratic closure, a quadratic closure with finite molecular aspect ratio, the two Hinch–Leal closures, a hybrid between the quadratic and the first Hinch–Leal closures and a recently proposed Bingham closure. The first part of the article studies the predictions of the models in homogeneous flows. We generate their bifurcation diagrams in the (U,Pe) plane, where U is the nematic strength and Pe is the Peclet number, and place special emphasis on the effects of the flow type. These solutions are then compared with the ''exact solutions'' of the unapproximated Doi theory. Results show the Bingham closure to give the best approximation to the Doi theory in terms of reproducing transitions between the director aligning, wagging and tumbling regimes at the correct values of U and Pe and predicting the arrest of periodic solutions by a mildly extensional flow. In the second part of the article, we employ the closure models to compute a complex flow in an eccentric cylinder geometry. All the models tested predict the same qualitative features of the LCP dynamics. Upon closer inspection of the quantitative differences among the solutions, the Bingham closure appears to be the most accurate. Based on these results, we recommend using the Bingham closure in simulating complex flows of LCPs. © *1998 The Society of Rheology.* [S0148-6055(98)01705-2]

I. INTRODUCTION

The interest in simulating complex flows of liquid-crystalline polymers (LCPs) comes mainly from the potential of injection molding such materials into high strength parts. For the flow and rheology of LCPs, the prevalent theoretical model is the Doi theory for rigid rod molecules [Doi (1981)]. When applied to nonhomogeneous flows, the Doi theory needs to be simplified by using closure approximations; solving the kinetic equation for the orientation distribution function in complex flows currently presents formidable difficulties [Armstrong *et al.* (1996); Nayak *et al.* (1997)]. Even after this task becomes commonplace, the huge savings in effort by using closure approximations will certainly make the latter more attractive in process design. Recently, Marrucci and Greco (1992) attempted to generalize the Doi theory by allowing nonlocal nematic interactions. This new feature is fundamentally important and its implementation at present seems possible only within the framework of the closure-approximated Doi theory.

[a)]Author to whom all correspondence should be addressed; Electronic mail: 19120@engineering.ucsb.edu

A number of closure approximations have appeared in the literature, the most familiar ones being the quadratic closure [Doi (1981)] and the Hinch–Leal closures [Hinch and Leal (1976)]. Recently, a Bingham closure was proposed by Chaubal and Leal (1998). The central issue in previous research on closure approximations is tumbling of the director in shear flows. In extension-dominated flows, the LCP director aligns steadily with the flow. The simple quadratic closure has proved to be sufficient for such flows [Ramalingam and Armstrong (1993); Mori *et al.* (1997)], although elaborate treatment of other closure models is available [Wang (1997)]. However, the quadratic closure fails to predict any periodic director motion in simple shear. The Hinch–Leal closures do predict director wagging and tumbling, but they yield pathological results at high Peclet number [Advani and Tucker (1990); Chaubal *et al.* (1995)]. The Bingham closure differs from the others in that it assumes a special form of the orientation distribution function—the Bingham distribution—based on which the relationship between the second and fourth moment tensors is established. This guarantees that the resulting closure never behaves pathologically. Comparison with the unapproximated solution in homogeneous flows shows good agreement for a wide range of parameters.

The quadratic closure is the only one that has been used in computing nonhomogeneous flows. In extension-dominated flows, the quadratic closure gives a good representation of the polymer configuration [Ramalingam and Armstrong (1993); Forest *et al.* (1997); Mori *et al.* (1997)]. Its use in pressure-driven channel flows, however, is questionable. The few studies to date all reported steady aligned solutions [Armstrong *et al.* (1995); Mori *et al.* (1995); Wang *et al.* (1996)]. In the flow between rotating eccentric cylinders, Feng and Leal (1997) observed director tumbling, wagging and alignment in different regions of the flow field. Most interestingly, their results suggest that director tumbling may be a cause of disclinations in nonhomogeneous flows. This role of director tumbling imparts additional significance to the choice of closure models for complex flows. The motivation for the current study is to examine a number of closure models in homogeneous and nonhomogeneous flows, in anticipation of using such closures for computational studies of director tumbling and disclination formation in complex flows.

We will begin with a comprehensive study of closure approximations in two-dimensional homogeneous flows. This is then followed by a comparison of model predictions in a specific inhomogeneous flow. Previous work in this area was done largely without the perspective of complex flow calculations. For instance, the effect of tube dilation on the rotational diffusivity has always been neglected. In a nonhomogeneous flow, tube dilation may have an important impact owing to the spatial variation of the order parameter [Feng and Leal (1997)]. From our viewpoint, the most basic features of a closure model are depicted in a solution diagram which illustrates stable regimes of director aligning, wagging and tumbling in various ranges of the nematic strength parameter U and the Peclet number Pe. Such diagrams are currently available only for the quadratic closure [Bhave *et al.* (1993)] and the first Hinch–Leal closure [Chaubal *et al.* (1995)], and effects of the flow type have not been systematically documented. In the first part of this study, we will generate solution diagrams in two-dimensional homogeneous flows for six closure models as well as the Doi theory without any closure approximation. All of the closures are described in Sec. II. Tube dilation is included and the effects of flow type are considered at length. Comparison of the solution diagrams for various closure models and for the exact theory will demonstrate their respective merits and deficiencies.

Observations in homogeneous flows may not carry over to nonhomogeneous flows for microstructured materials. The LCP configuration at a certain point is not determined solely by the local strain rate and flow type; the flow and deformation history along the

streamline leading to this point play an essential role [Szeri *et al.* (1991); Feng and Leal (1997)]. Therefore, in a complex flow, the spatially varying flow conditions may diminish or accentuate the differences among closure models observed in homogeneous flows. We will numerically simulate the nonhomogeneous flow in an eccentric-cylinder flow device using the closure models. This geometry produces extensional, shear and rotational flows in various regions of the domain, and therefore suits our purpose well. The numerical simulations in this article seem to represent the first flow calculations done for any closure models except the quadratic closure. As mentioned before, flow calculations using the exact Doi theory are improbable at this stage, so we are unable to compare the predictions of the closure models with that of the exact theory in the nonhomogeneous flow.

II. THE CLOSURE MODELS

This section briefly describes the Doi theory and the closure models to be discussed in the rest of the article. The Doi theory is based on an orientation distribution function $\Psi(\mathbf{u})$ for an ensemble of rigid rods, $\mathbf{u}$ being the unit vector along each rod. Following the Prager procedure, the evolution equation of the second moment tensor $\mathbf{A} = \int \mathbf{uu}\Psi(\mathbf{u})d\mathbf{u} = \langle \mathbf{uu} \rangle$ can be derived:

$$\frac{\partial \mathbf{A}}{\partial t} + \mathbf{v}\cdot\nabla\mathbf{A} - \nabla\mathbf{v}^T\cdot\mathbf{A} - \mathbf{A}\cdot\nabla\mathbf{v} = -\frac{f}{\mathrm{Pe}}\left(\mathbf{A} - \frac{\boldsymbol{\delta}}{3}\right) + \frac{fU}{\mathrm{Pe}}(\mathbf{A}\cdot\mathbf{A} - \mathbf{A}:\langle \mathbf{uuuu} \rangle) - 2\mathbf{D}:\langle \mathbf{uuuu} \rangle, \tag{1}$$

where δ is the unit tensor, $\mathbf{v}$ is the fluid velocity and $\mathbf{D} = (\nabla\mathbf{v} + \nabla\mathbf{v}^T)/2$. The Peclet number $\mathrm{Pe} = \Gamma/(6D_r)$ is defined using a characteristic strain rate Γ and the rotational diffusivity D_r in an isotropic solution of the same volume concentration. U is the nematic strength in the Maier–Saupe potential and f represents the tube dilation effect, i.e., the enhancement in rotational diffusion due to the nematic molecular order. The polymer stress may be written as

$$t = \left(\mathbf{A} - \frac{\delta}{3}\right) - U(\mathbf{A}\cdot\mathbf{A} - \mathbf{A}:\langle \mathbf{uuuu} \rangle) + \frac{\beta \mathrm{Pe}}{(\nu L^3)^2}\mathbf{D}:\langle \mathbf{uuuu} \rangle, \tag{2}$$

where τ has been scaled by $3\nu kT$, ν being the volume concentration of the LCP solution, k the Boltzmann constant and T the temperature. L is the length of the rods, $(\nu L^3)^2$ is the crowdedness factor and $\beta = O(10^3)$ is an empirical parameter. Note that in deriving (1), the motion of an LCP molecule is taken to be that of a thin rod of infinite aspect ratio.

The above equations differ slightly from the original formulations of Doi (1981). The $(\mathbf{v}\cdot\nabla\mathbf{A})$ term in Eq. (1) is added to describe the variation of $\mathbf{A}$ along a streamline in a nonhomogeneous flow [Feng and Leal (1997)]. The last term in Eq. (2) is a viscous stress originally omitted by Doi (1981). It is important at high flow rates [see, e.g., Marrucci and Maffettone (1989)] and thus retained here.

In order to ''close'' the theory at the level of the second moment tensor $\mathbf{A} = \langle \mathbf{uu} \rangle$, f and $\langle \mathbf{uuuu} \rangle$ need to be expressed in terms of $\mathbf{A}$. Doi (1981) has suggested a simple form for the tube dilation effect:

$$f = (1 - S^2)^{-2} = \tfrac{4}{9}(1 - \mathbf{A}:\mathbf{A})^{-2}, \tag{3}$$

where $S = [(3\mathbf{A}:\mathbf{A}\text{-}1)/2]^{1/2}$ is the order parameter. We will use this form in this article. The relationship between $\langle \mathbf{uuuu} \rangle$ and $\langle \mathbf{uu} \rangle$ is represented by the various closure models.

A. The quadratic closure

The simplest and most widely used approximation is the quadratic closure originally adopted by Doi (1981):

$$\langle \mathbf{uuuu} \rangle = \langle \mathbf{uu} \rangle \langle \mathbf{uu} \rangle = \mathbf{AA}. \tag{4}$$

Here, the fourth moment tensor is replaced by **AA** when contracting into **A** and **D** in Eqs. (1) and (2). The quadratic closure fails to reproduce director tumbling and wagging in simple shear flow, as predicted by the exact (i.e., unapproximated) Doi theory.

B. The QuadR closure

The Doi theory models LCP molecules as rods of infinite aspect ratio. In a simple shear flow, such a rod tends to align with the flow. Brownian diffusion constantly kicks individual rods out of alignment with the flow. The rods then rotate back to the aligned state, but in the absence of nematic interaction the distribution function would remain time independent. The cohesive force due to nematic interaction allows for collective rotation of the rods for some ranges of Pe and U, and hence director tumbling in simple shear flow. This is the result of a delicate balance between the tendency of the strain rate **D** to maintain a fixed orientation and the tendency of the vorticity $\mathbf{\Omega}$ to induce rotation. The quadratic closure approximation of the term $\mathbf{D}:\langle \mathbf{uuuu} \rangle$ in Eq. (1) leads to a slight overestimate of the strain-rate effect as compared to the vorticity effect, and hence shifts the balance in the quadratic closure based model so that no director tumbling occurs in simple shear. In fact, the tendency for tumbling is recovered for flows that are slightly more rotational than simple shear [Chaubal *et al.* (1995)]. It may also be recovered, as explained below, by modifying Eq. (1) to a form that would be appropriate for rods of a finite aspect ratio.

A cylindrical rod of an ''effective aspect ratio'' r_e [Anczurowski and Mason (1968)] rotates in a simple shear flow along a Jeffery orbit:

$$\dot{\mathbf{u}} = \mathbf{\Omega} \cdot \mathbf{u} + \lambda (\mathbf{D} \cdot \mathbf{u} - \mathbf{D}:\mathbf{uuu}), \tag{5}$$

where $\mathbf{\Omega}$ and **D** are the vorticity and the rate-of-deformation tensors. The parameter λ is related to r_e: $\lambda = (r_e^2 - 1)/(r_e^2 + 1)$. Hence, a decrease of r_e from infinity to a finite value reduces the relative strength of the strain rate with respect to the vorticity in determining the rotation of a rodlike molecule. The collective behavior of an ensemble of rods is similarly modified by the finite aspect ratio; the evolution equation of **A** becomes

$$\frac{\partial \mathbf{A}}{\partial t} + \mathbf{v} \cdot \nabla \mathbf{A} = (\mathbf{\Omega} + \lambda \mathbf{D}) \cdot \mathbf{A} + \mathbf{A} \cdot (-\mathbf{\Omega} + \lambda \mathbf{D}) - 2\lambda \mathbf{D}:\langle \mathbf{uuuu} \rangle - \frac{f}{\mathrm{Pe}} \left(\mathbf{A} - \frac{\boldsymbol{\delta}}{3} \right)$$

$$+ \frac{fU}{\mathrm{Pe}} (\mathbf{A} \cdot \mathbf{A} - \mathbf{A}:\langle \mathbf{uuuu} \rangle). \tag{6}$$

The behavior of a nematic solution of rods of finite aspect ratio is then equivalent to that of the original infinite-aspect-ratio system in a more rotational flow. Indeed, one may think of the effect of the finite aspect ratio as changing the flow type parameter from α [see Astarita (1979) for definition] to

$$\tilde{\alpha} = \frac{\lambda |\mathbf{D}| - |\mathbf{\Omega}|}{\lambda |\mathbf{D}| + |\mathbf{\Omega}|} = \frac{\lambda (1 + \alpha) - (1 - \alpha)}{\lambda (1 + \alpha) + (1 - \alpha)}. \tag{7}$$

If we replace $\langle \mathbf{uuuu} \rangle$ in (6) by **AA** and use a λ value less than unity, the overestimate of the strain-rate effect by the quadratic closure may be compensated so that the predic-

tions of the model, hereafter called QuadR, provide a better approximation to the dynamics of **A** as predicted by the original Doi model with no closure and an infinite molecular aspect ratio. In this framework, the parameter r_e is viewed as ''ad hoc,'' chosen to give the best approximation to the unapproximated Doi theory rather than having any relation to the actual shape of the LCP molecule. Equation (2) for the stress remains unaltered because it is still the infinite-aspect-ratio Doi theory that we are trying to approximate. The fourth moment terms in this equation are calculated from **A** via the quadratic closure approximation [Eq. (4)].

C. The HL1 and HL2 closures

Hinch and Leal (1976) proposed two closures based on interpolating between the weak and strong flow limits in a Brownian suspension of rods. The HL1 closure can be written as

$$\mathbf{B}:\langle\mathbf{uuuu}\rangle = \tfrac{1}{5}[6\mathbf{A}\cdot\mathbf{B}\cdot\mathbf{A}-\mathbf{B}:\mathbf{AA}+2\boldsymbol{\delta}(\mathbf{A}-\mathbf{A}\cdot\mathbf{A}):\mathbf{B}], \tag{8}$$

and the HL2 closure as:

$$\mathbf{B}:\langle\mathbf{uuuu}\rangle = \mathbf{AA}:\mathbf{B}+2\mathbf{A}\cdot\mathbf{B}\cdot\mathbf{A}-\frac{2\mathbf{A}\cdot\mathbf{A}:\mathbf{D}}{\mathbf{A}:\mathbf{A}} \times\mathbf{A}\cdot\mathbf{A}+\rho\left[\frac{52}{315}\mathbf{B}-\frac{8}{21}\left(\mathbf{B}\cdot\mathbf{A}+\mathbf{A}\cdot\mathbf{B}-\frac{2}{3}\mathbf{A}:\mathbf{B}\boldsymbol{\delta}\right)\right], \tag{9}$$

where $\rho = \exp[(2-6\mathbf{A}:\mathbf{A})/(1-\mathbf{A}:\mathbf{A})]$. In Eqs. (8) and (9), **B** is any traceless tensor. These relationships can be applied directly to $\mathbf{D}:\langle\mathbf{uuuu}\rangle$. The $\mathbf{A}:\langle\mathbf{uuuu}\rangle$ term can be worked out by replacing **B** by the traceless $\mathbf{A}-\boldsymbol{\delta}/3$.

D. The HL1Q closure

It has been noted that the accuracy of a closure model differs considerably when applied to the ''nematic term'' $\mathbf{A}:\langle\mathbf{uuuu}\rangle$ and the ''flow term'' $\mathbf{D}:\langle\mathbf{uuuu}\rangle$ [Larson and Mead (1991); Baek *et al.* (1993)]. The quadratic closure is generally accurate for the nematic term. It is its inaccuracy in the flow term that causes the loss of periodic solutions in simple shear. Numerical experiments by Chaubal (1997) showed that the HL1 closure is more accurate than the quadratic closure for the flow term, but the reverse is true for the nematic term. It is then natural to propose a hybrid model using the quadratic closure for $\mathbf{A}:\langle\mathbf{uuuu}\rangle$ and the HL1 closure for $\mathbf{D}:\langle\mathbf{uuuu}\rangle$. We denote the resulting model as the HL1Q closure.

E. The Bingham closure

The Bingham closure is based on the idea that $\langle\mathbf{uuuu}\rangle$ can be related to $\langle\mathbf{uu}\rangle$ by assuming a special form for the orientation distribution function. Chaubal and Leal (1998) chose the Bingham distribution:

$$\Psi(\mathbf{u}) = \frac{1}{Z}\exp(\mathbf{u}\cdot\mathbf{T}\cdot\mathbf{u}), \tag{10}$$

where **T** is a symmetric matrix and Z is a normalization constant. Owing to the orthotropy of the fourth moment tensor $\langle\mathbf{uuuu}\rangle$ [Cintra and Tucker (1995)], the number of its independent components is greatly reduced in its principal coordinate system. These independent components can be related to the eigenvalues of $\langle\mathbf{uu}\rangle$ through integration over the Bingham distribution function. For the ease of implementation, Chaubal and

Leal (1998) established this relationship by fitting third-order polynomials to calculated values of the independent components of $\langle \mathbf{uuuu} \rangle$ for 284 pairs of eigenvalues of $\langle \mathbf{uu} \rangle$ that were chosen to cover the full range of realizable values.

The Bingham closure is built on a distribution function that is symmetric about three orthogonal planes containing the principal axes of **T**. Therefore, it is exact in the weak flow limit (i.e., the equilibrium state) and in potential flows. Its accuracy is expected to decline in flows that skew the distribution function. A salient feature of the Bingham closure is that it never produces pathological predictions. This is owing to the fact that the $\langle \mathbf{uuuu} \rangle$ components are calculated using a physically acceptable orientation distribution function, albeit one which may be an inaccurate approximation in some regions of the parameter space.

III. HOMOGENEOUS FLOWS

In this section we compare solutions of the Doi theory in two-dimensional homogeneous flows with and without a closure approximation. The dimensionless velocity gradient tensor is:

$$\nabla \mathbf{v} = \begin{bmatrix} 0 & \alpha & 0 \\ 1 & 0 & 0 \\ 0 & 0 & 0 \end{bmatrix}, \tag{11}$$

where α is the flow type parameter. We assume that the director orientation is symmetric with respect to the flow plane, and therefore exclude director kayaking from this work. Kayaking is a rather exceptional regime of director motion [Larson and Öttinger (1991)] and its inclusion would make the inhomogeneous flow calculation of Sec. IV three dimensional and much more costly. Under the current assumption,

$$\mathbf{A} = \begin{bmatrix} a_1 & a_2 & 0 \\ a_2 & a_3 & 0 \\ 0 & 0 & 1-a_1-a_3 \end{bmatrix}. \tag{12}$$

With a closure approximation, Eq. (1) [or Eq. (6) for the QuadR model] can be broken down to three coupled ordinary differential equations for the three unknown components of **A**, which are then solved using a fourth-order Runge–Kutta method with automatic time step adjustment. In-plane orientations are always used as initial conditions.

Solving the unapproximated Doi theory is a much more elaborate endeavor. We use a smoothed-particle-hydrodynamics algorithm to compute the evolution of the orientation distribution function in the same homogeneous flows. Details of the method have been described elsewhere [Chaubal *et al.* (1997)].

A. The quadratic and QuadR closures

As explained in the last section, the QuadR model gives the same results as the original Doi theory with the quadratic closure in a flow that is effectively more rotational. Therefore, the solution diagrams for the quadratic closure and the QuadR model are the same subject to a change of the flow type parameter. Figure 1 shows the results for the quadratic closure.

The structure of this diagram is well known from the previous study of Chaubal *et al.* (1995). For a *negative* value of the flow type parameter α, director aligning, wagging and tumbling occur in three domains delineated by three curves in the (U,Pe) plane. The vertical line at small Pe (curve a) marks a homoclinic bifurcation; the director aligns with

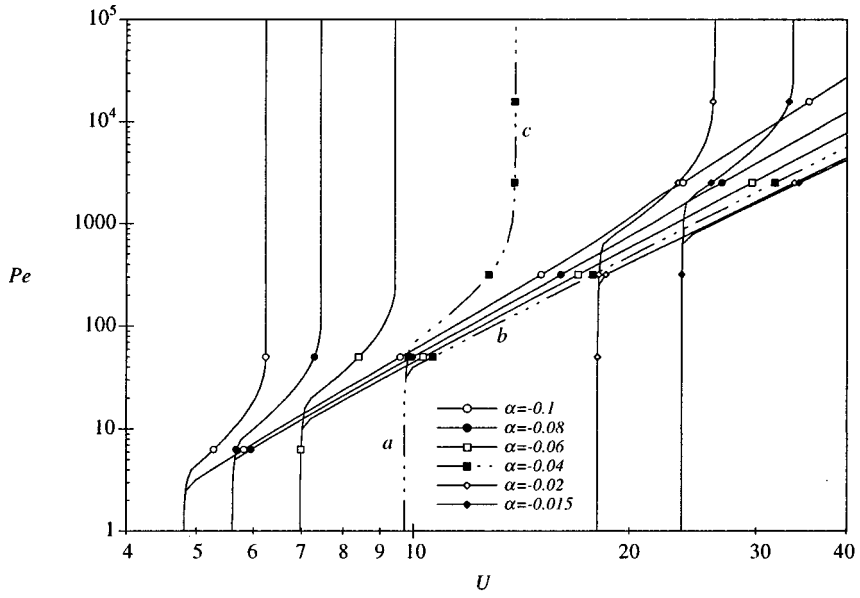

FIG. 1. Solution diagram of the quadratic closure in homogeneous flows of flow type parameter α. As an example, the broken curves a, b and c mark the boundaries of different regimes of director motion for $a = -0.04$. All curves are bounded on the left by the critical U for the isotropic–nematic transition.

the flow on the left side of curve a and tumbles on the right. Curve b is the ceiling of the tumbling domain, above which director wagging prevails. Curve c indicates a Hopf bifurcation that demarcates flow aligning (which occurs above and to the left of curve c) and wagging solutions. Curves a and b are determined numerically by bisecting an interval of U for a fixed Pe. Curve c is computed semianalytically by studying the Jacobian of the linearized differential equations and finding the critical point where the real part of the eigenvalues changes sign. The same scheme is used for the HL and HL1Q closures to be presented below. For the Bingham closure and the exact Doi theory, the numerical approach is used to compute all three curves.

With increasing α, all three curves shift to the upper right of the diagram; the tumbling and wagging domains recede to the right but never disappear completely for any $\alpha < 0$. The curve c for the Hopf bifurcation becomes a vertical line at a large Peclet number. Therefore, based on the quadratic closure, wagging will not be suppressed by increasing the flow rate if the nematic order is sufficiently strong. This will be seen to be an artifact that all the closure models incur.

We emphasize that the prediction of the QuadR model is precisely the same as shown in Fig. 1, but with the effective flow type parameter of Eq. (7) replacing α. Now a value of the nominal aspect ratio can be chosen such that tumbling occurs in a simple shear flow for the QuadR model.

B. The HL1 closure

The solution diagram for the HL1 closure has a similar structure (Fig. 2), except that HL1 admits a periodic solution for $\alpha = 0$ as well as slightly positive flow type parameters. As α increases, the flow-aligning regime encroaches on the domain of periodic solutions from the left. Interestingly, there appears to be another boundary on the right (curve d), beyond which the solution is again flow aligning. Curve d, almost vertical in

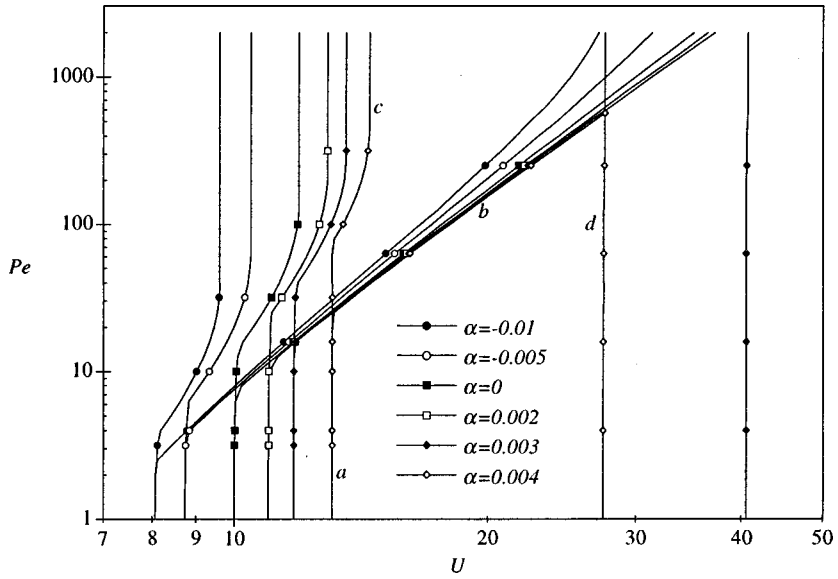

FIG. 2. Solution diagram of the HL1 closure. Taking $\alpha = 0.04$ as an example, curves *a*, *b*, *c* and *d* demarcate different regimes of director motion.

Fig. 2, represents a second homoclinic bifurcation; the period of the tumbling solution or wagging solution goes to infinity as one approaches this boundary from the left. With increasing α, curve *d* moves to the left and so the tumbling and wagging domains are squeezed from both sides. This is how the extensional character of the flow eliminates periodic solutions.

The solution structure for $\alpha > 0$ with a tumbling domain sandwiched between flow-aligning domains at large and small values of U is inherent in the *unapproximated* Doi theory; it is distorted by the quadratic closure but remains with the HL1 closure. The origin of this behavior can be understood in the limit of weak flows. The Doi theory then reduces to the Leslie–Ericksen theory, and the motion of the director **n** in a homogeneous flow follows:

$$\frac{\partial \mathbf{n}}{\partial t} = \mathbf{\Omega}\cdot\mathbf{n} + \lambda(\mathbf{D}\cdot\mathbf{n} - \mathbf{D}\!:\!\mathbf{nnn}), \tag{13}$$

where the tumbling parameter λ depends on the nematic strength U but not on the flow. Without closure approximation, Kuzuu and Doi (1984) calculated the tumbling parameter using the Onsager potential and Archer and Larson (1995) did the same with the Maier–Saupe potential. With closure approximations, λ is much easier to calculate [Larson (1990)]. Figure 3 compares predictions of λ as a function of U for the various closure models with the results of Archer and Larson (1995). In a simple shear flow, the director aligns with the flow for $\lambda > 1$ and tumbles for $\lambda < 1$. The exact curve and the HL1 curve both have a valley in which $\lambda < 1$, signifying director tumbling in simple shear over most of the U values for which there is a nematic phase. In a *nonshear* two-dimensional flow characterized by flow type parameter α, the director tumbles if

$$\lambda < \frac{1-\alpha}{1+\alpha}. \tag{14}$$

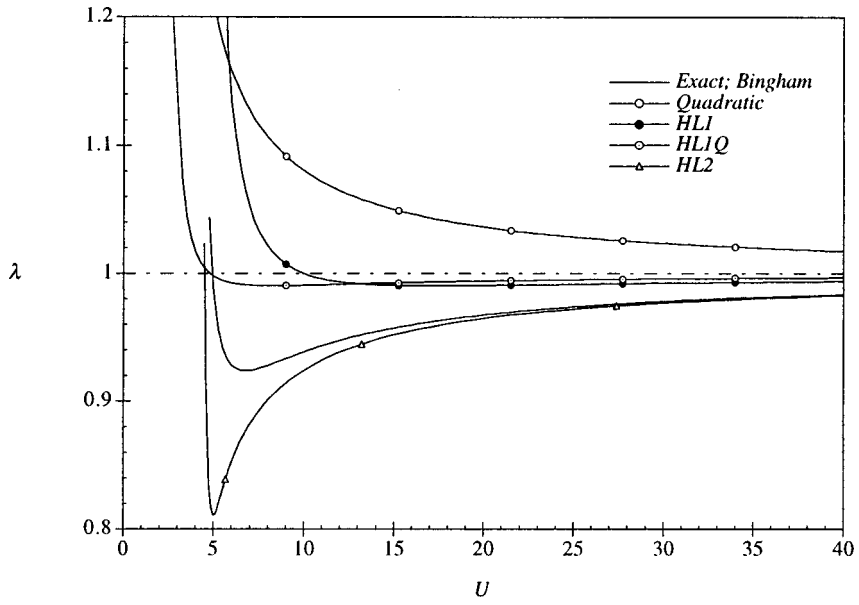

FIG. 3. Comparison of the tumbling parameter λ for the unapproximated Doi theory and the closure models. All curves converge to $\lambda = 1$ as U tends to infinity. The minimum U for a stable nematic phase is 4.898 for the HL1 closure, 4.457 for the HL2 closure, 4.55 for the unapproximated theory and the Bingham closure and 2.667 for the quadratic and HL1Q closures. The HL1Q, Bingham and HL2 curves are discussed later in this section.

This can be easily seen by manipulating the relative magnitudes of $\mathbf{\Omega}$ and $\mathbf{D}$ in Eq. (13), which holds for any planar homogeneous flow. For a positive α, it can be seen from Fig. 3 and Eq. (14), that the tumbling domain shrinks from both sides for the unapproximated theory and for all closure models except the quadratic closure. For the quadratic model, $\lambda > 1$ and thus director tumbling occurs only for $\alpha < 0$. When the negative α increases, Fig. 3 shows that the tumbling domain will shrink only from the left side as occurs in Fig. 1. One also notes that the exact theory has a significantly deeper valley (in which $\lambda < 1$) than all closure models except HL2. Thus, for most of the closure-based models, the range of α in which periodic solutions are predicted by Eq. (13) is much smaller than it is for the exact theory. HL2 is an exception in that tumbling persists to higher α values than for the exact theory. Although the above arguments are based on the weak flow limit, they appear to apply qualitatively to moderate and large Pe in Figs. 1 and 2.

Roughly speaking, the effect of tube dilation on the solution diagrams is to move the curves to larger Peclet numbers; Figs. 1 and 2 can be compared with the diagrams in Chaubal *et al.* (1995). This is because the enhanced molecular diffusion is tantamount to reduced flow strength. Since the order parameter S varies periodically during wagging and tumbling, the tube dilation effect is in fact rather subtle and cannot be simply represented by a change in Pe.

Finally, we note an aphysical behavior of the HL1 closure first pointed out by Chaubal *et al.* (1995). The order parameter fails to approach unity as $\mathrm{Pe} \to \infty$; instead S tends to a constant $S_\infty < 1$ (for wagging solutions, the mean of S approaches S_∞). S_∞ assumes the value of $\sqrt{7/12}$ in simple shear and appears to increase monotonically toward unity with increase of the flow type α.

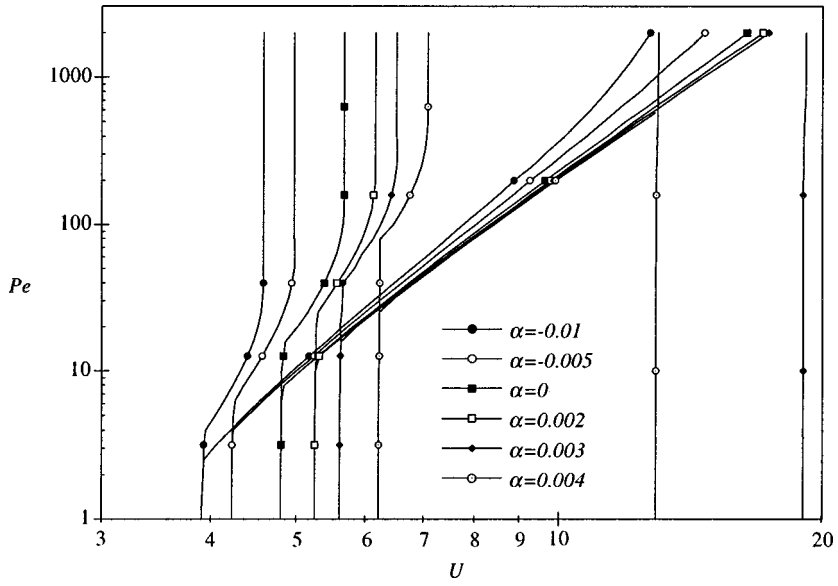

FIG. 4. Solution diagram of the HL1Q closure.

C. The HL1Q closure

The solution diagram for the HL1Q closure is very similar to that of the HL1 closure, except that all the curves appear shifted to lower U values (Fig. 4). The reason for this nearly uniform shift can again be understood from the weak flow limit.

The only difference between the HL1 and HL1Q closures is in the nematic term $\mathbf{A}:\langle\mathbf{uuuu}\rangle$. Since the Brownian term and the nematic term cancel exactly in the absence of flow, the motion of the director in the weak flow limit ($\mathrm{Pe} \to 0$) is the same for the two closures when expressed in terms of the equilibrium order parameter S_{eq} [Larson (1990)]. But S_{eq} as a function of U depends on the form of the nematic term, hence the shifts of critical U values for transitions in the solution. More precisely, the critical U at the first homoclinic bifurcation is related for the two closures by

$$S_{\mathrm{eq}}^{c} = \frac{1}{4}\left(1+\sqrt{9-\frac{24}{U_{\mathrm{HL1Q}}}}\right) = \frac{1}{8}\left(1+\sqrt{49-\frac{240}{U_{\mathrm{HL1}}}}\right). \tag{15}$$

The HL1 and HL1Q curves in Fig. 3 also observe this relationship, and the homoclinic bifurcation is where the curves intersect $\lambda = 1$. For a finite Pe, the relationship between the two closures may be more complex than the simple shift indicated by Eq. (14), but a degree of parallelism remains.

D. The Bingham closure

The solution diagram for the Bingham closure has a structure similar to those discussed above (Fig. 5). The locus of the Hopf bifurcation, marking the boundary between flow aligning and wagging solutions, are difficult to determine at large Pe. As mentioned before, this curve is computed numerically by bisecting an interval of U based on the predicted behavior at the two ends of the interval. At high Pe, the solution has long transients and even a flow-aligning solution may appear as wagging after a long but finite period of time. Any flow-aligning criterion based on the finite-time behavior is necessar-

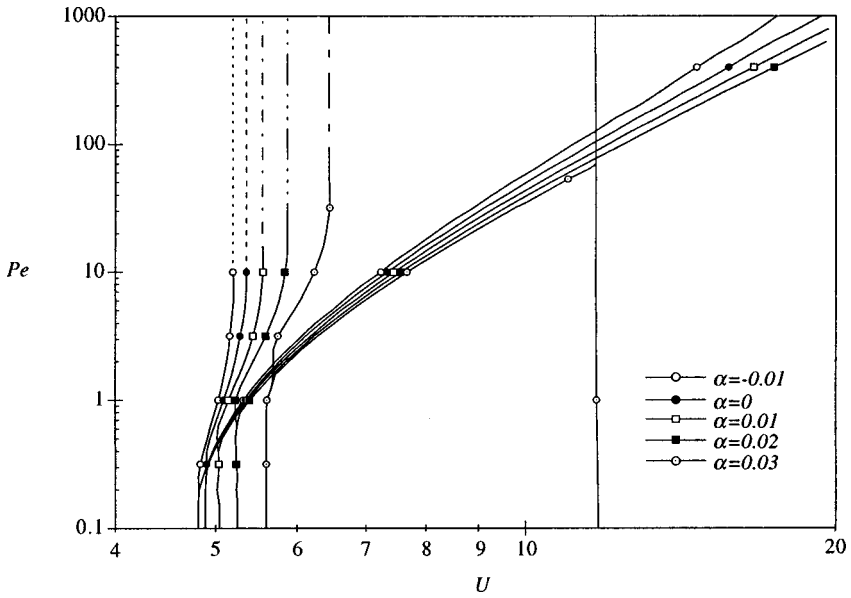

FIG. 5. Solution diagram of the Bingham closure. For $\alpha \geqslant 0.04$, no periodic solution can be found in the (U,Pe) ranges studied.

ily arbitrary. Thus we draw the upper part of the aligning–wagging boundary as dashed lines in Fig. 5 following the patterns in Figs. 2 and 4. For Pe smaller than about 10, the margin of error in determining the locus of the Hopf bifurcation is rather small.

Two features of Fig. 5 stand out. First, the behavior of the director, as predicted by the Bingham closure, is far less sensitive to the flow type parameter α than for the three models discussed above. For the range of α values tested, the spread of the curves is much smaller in Fig. 5 than in Figs. 1, 2 and 4. This can also be inferred from the shape of the curves in Fig. 3; at their respective intersections with $\lambda = 1$, the Bingham curve has the steepest slope among the closure models (except HL2; see below). Hence the critical U for the aligning–tumbling transition will shift the least for the Bingham curve when the flow type is varied. Periodic solutions are arrested by extensional flows in the same fashion for the Bingham, the HL1 and the HL1Q closures, but they persist to a significantly larger α for the Bingham model, as is also true for the unapproximated Doi theory. Second, the curves in Fig. 5 appear to be shifted downward as compared to Figs. 2 and 4; transitions in the solution occur at smaller critical Pe values.

E. The HL2 closure

As alluded to in the preceding discussions, HL2 stands apart from the other closure models in several aspects. At the weak flow limit (Fig. 3), HL2 is the only closure that has a stronger tendency toward director tumbling than the exact Doi theory. Also at the intersection with $\lambda = 1$, the HL2 curve is the only one that has a slope steeper than the exact curve. Hence, HL2 is the least sensitive to the flow type at the weak flow limit; the critical U corresponding to the homoclinic bifurcation shifts the least as α varies.

The solution diagram of HL2 also has some peculiar features (Fig. 6). The wagging–tumbling boundary bends to the left for large Pe. Therefore, for sufficiently large U, director tumbling will not be suppressed by high Pe in simple shear. For smaller U, the wagging amplitude increases with Pe and wagging may eventually become tumbling.

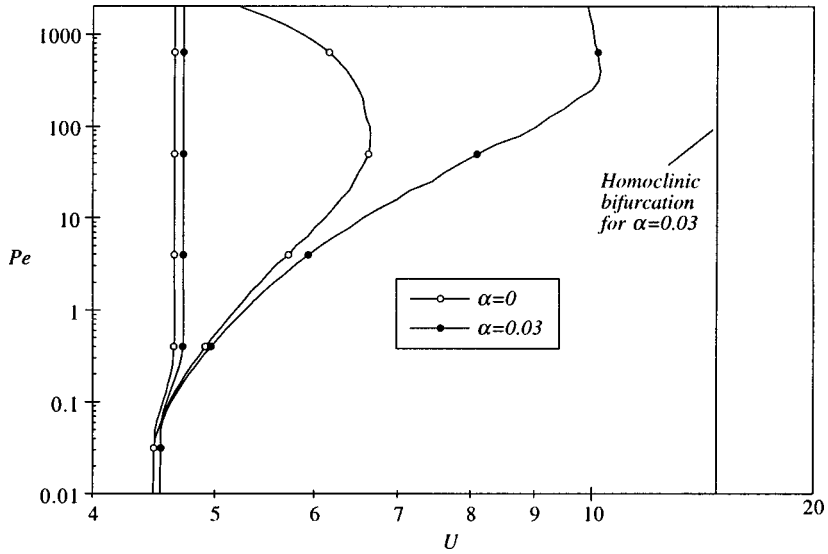

FIG. 6. Solution diagram of the HL2 closure.

When applied to Brownian suspensions of rods, HL2 has a well-known failing: it predicts spurious oscillations in shear flows at high Pe [Advani and Tucker (1990); Szeri and Lin (1996)]. Evidently Fig. 6 manifests the same failing. In fact, a nematic solution becomes indistinguishable from a suspension of rodlike particles as Pe tends to infinity; see Eq. (1).

For positive α, a second homoclinic bifurcation occurs which bounds the tumbling domain on the right. From Fig. 3 and Eq. (13), one may estimate that at the weak flow limit, director tumbling will be suppressed only for $\alpha > 0.1$. Thus, at the weak flow limit, the HL2 closure is insensitive to α. For higher Pe, however, the wagging–tumbling boundary varies greatly with α.

F. Comparison and discussion

Having constructed solution diagrams for all the closure models in homogeneous flows, we now undertake a more detailed comparison among them as well as a direct comparison with the predictions of the unapproximated Doi theory. We will concentrate on three characteristics of the solution diagrams: the critical U values where transitions in the solution occur, particularly the critical U_h for the first homoclinic bifurcation; the critical Pe values where transitions occur; and finally the reaction of the model predictions to the flow type parameter α.

Figure 7 compares the solution diagrams of various closure models and the exact Doi theory for a simple shear flow. The quadratic closure predicts no transition from flow aligning at any U or Pe and thus does not appear. In order to use the QuadR model, a nominal molecular aspect ratio r_e has to be chosen. We have taken $r_e = \sqrt{10}$ so that in a simple shear flow, $\tilde{\alpha} = -0.1$ and the QuadR model predicts a homoclinic bifurcation that is fairly close to that of the exact theory [Fig. 7(b)]. Incidentally, this ad hoc r_e value is an order of magnitude smaller than the typical aspect ratio of real LCP molecules [Donald and Windle (1992); Walker and Wagner (1994)].

The behavior of the HL2 closure deviates markedly from the exact theory [Fig. 7(a)]. In its original context of Brownian suspensions of rods, HL2 represents a higher-order

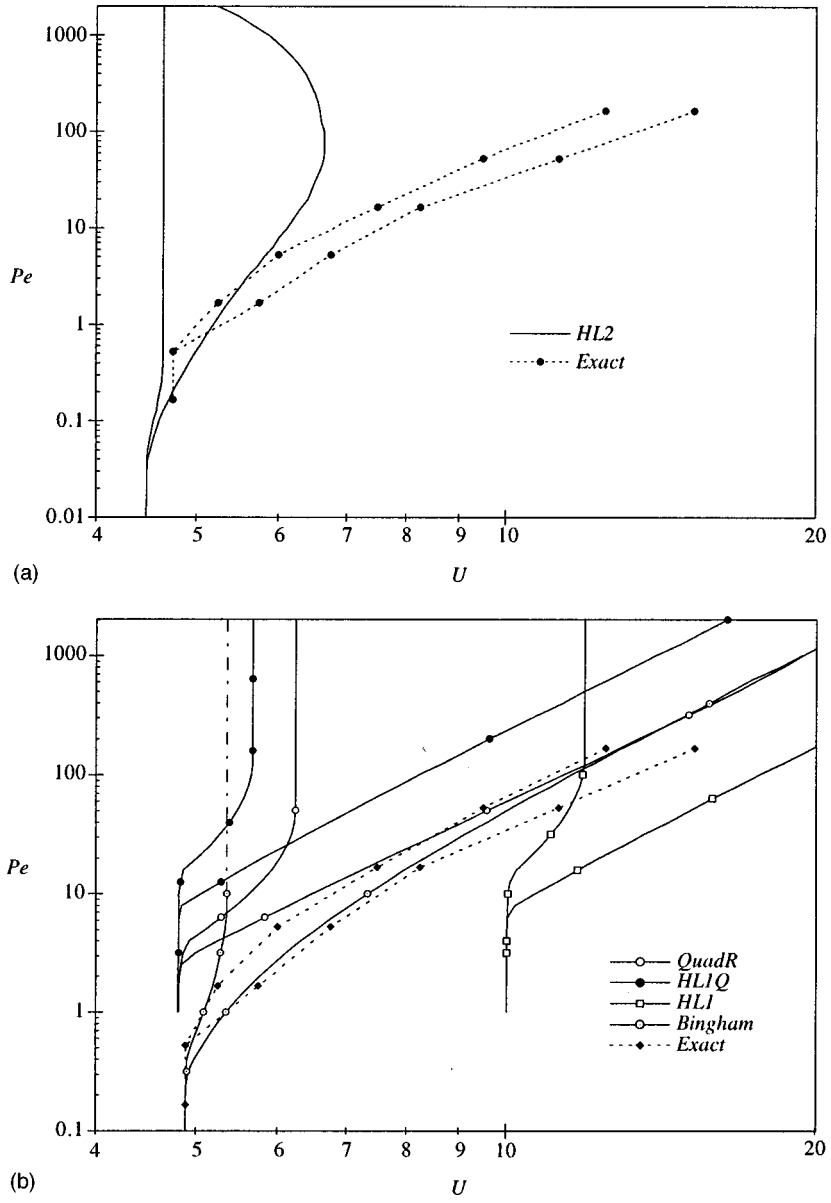

FIG. 7. Comparison of the solution diagrams of closure models and the unapproximated Doi theory in a simple shear flow. (a) The HL2 closure and the exact theory; (b) the other closures. For QuadR, a nominal molecular aspect ratio $r_e = \sqrt{10}$ is used.

approximation than HL1 [Hinch and Leal (1976)]. Then one may expect HL2 to be more accurate for LCPs as well. In the weak flow limit this is arguably true (see Fig. 3). For Pe above 1, however, HL2 exhibits an exceedingly strong tendency toward director tumbling, and its solution diagram becomes qualitatively different from that of the unapproximated Doi theory.

A common failing of all the closures in Fig. 7 is in the Hopf bifurcation curves: for most values of U they predict a wagging regime that extends to arbitrarily large Pe. In particular, if U is sufficiently large, increasing Pe does not lead to a transition from

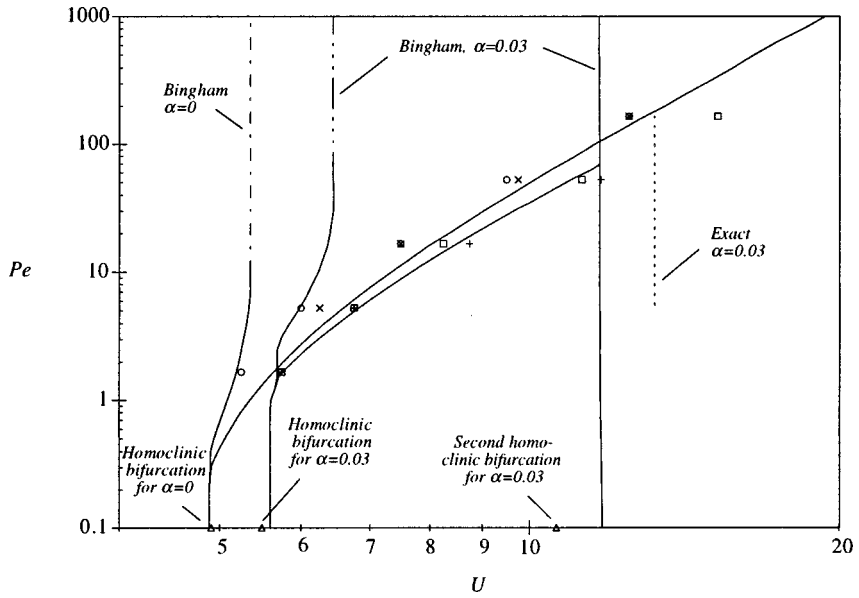

FIG. 8. Sensitivity of the Bingham closure and the unapproximated Doi theory to the flow type parameter α. Solid lines represent results of the Bingham closure for $\alpha = 0$ and 0.03. The circles represent the aligning-wagging boundary for the exact theory and the squares the tumbling-wagging boundary, both for $\alpha = 0$. The $\times$'s and crosses represent the two boundaries respectively for $\alpha = 0.03$ and the dash line on the right marks the second homoclinic bifurcation. The triangles on the U axis indicate the critical U_h for the homoclinic bifurcations in the Leslie–Ericksen limit.

wagging to flow aligning. In the exact theory, the boundary between aligning and wagging solutions does not become vertical at a high Peclet number but remains more or less parallel to the tumbling–wagging boundary. Thus, wagging can be suppressed at any U by increasing Pe. This confirms previous analysis on a two-dimensional version of the Doi theory in simple shear [Maffettone and Crescitelli (1994)].

The HL1 closure appears to be the least desirable of the closures shown in Fig. 7(b) in that the homoclinic bifurcation is predicted at too large a U_h value. This is a result of the HL1 closure underestimating the order parameter at equilibrium S_{eq}; also see Eq. (14). Because the Bingham distribution [Eq. (9)] is exact in the limit of weak flows, the Bingham closure exactly reproduces the tumbling parameter of the Doi theory (see Fig. 3), and in particular the critical U_h for the homoclinic bifurcation. The HL1Q model and the QuadR model, with the appropriately chosen r_e parameter, also give accurate predictions of U_h. Both models fail, however, to capture the boundary between tumbling and wagging; the critical Pe for arresting director tumbling is too large. In this regard, the Bingham model does well for smaller U, although the discrepancy seems to grow with U. On the whole, the Bingham closure appears to be the best in terms of approximating the exact solution diagram in the (U,Pe) plane. The QuadR closure is the second best, followed by the HL1Q, HL1 and HL2 models.

The effect the flow type parameter α is most interestingly manifested in arresting periodic director motions in extensional flows. All closure models except the QuadR closure have captured the essential features of this scenario. Figure 8 compares the Bingham closure and the exact theory in terms of their reaction to a mildly extensional flow. In the weak flow limit, the Bingham model converges to the exact theory, this common Leslie–Ericksen limit being denoted by triangles on the U axis. Away from that

limit, the Bingham closure is slightly more sensitive to α than the exact theory. As α changes from 0 to 0.03, the aligning–wagging boundary barely changes for the exact theory but changes appreciably for the Bingham model. The change in the tumbling–wagging boundary is comparable for the two. The second homoclinic bifurcation at large U, marking a tumbling–aligning transition, shifts more to the left for the Bingham closure. With an increasing α, therefore, the domains of wagging and tumbling contract more for the Bingham closure than for the exact theory. For the Bingham model, $\alpha = 0.04$ annihilates all periodic solutions within the parameter ranges studied ($\mathrm{Pe} \geqslant 0.1$); for the exact theory, periodic solutions persists to $\alpha = 0.05$. Incidentally, the Bingham curves in Fig. 8 do not go through the triangles; $\mathrm{Pe} = 0.1$ is apparently still too strong a flow.

For rotational flows ($\alpha < 0$), the Bingham closure approximates the exact theory extremely well, as it does in the opposite extreme of strongly extensional flows [Chaubal and Leal (1998)]. This is because the distribution function is not skewed seriously in rotational and nearly purely extensional flows. For intermediate flow conditions, the Bingham closure is the least sensitive of all the closure models (except perhaps HL2) and gives by far the best approximation. The artificial sensitivity of the other models to α can be appreciated in Figs. 1, 2 and 4.

To summarize the findings of this section, there are two shortcomings common to all of the closure models considered here; one is excessive sensitivity to the flow type and the other is the failure to arrest wagging at high Peclet numbers. The fact that none of the closure approximations correctly reproduces the transition between wagging and flow aligning may be intrinsic to closure at the second-moment level. Direct solutions of the distribution function Ψ [Chaubal and Leal (1998)] show that Ψ is skewed at the transition and hence cannot be faithfully represented by any second-moment approximation. Larson (1990) discovered, using the unapproximated Doi theory, that in steady alignment the normal stress differences undergo a sign change as Pe increases. Hence, the closure models may not produce the correct normal stresses at high Pe [Baek *et al.* (1993)]. This is a potentially serious drawback in simulating flow situations where the normal stresses play an important role. Of all the closure models considered, the Bingham closure gives the best performance on account of its approximation of the solution diagram in the (U,Pe) space for simple shear flows and its least sensitivity to the flow type. The other closures have additional problems: the QuadR closure fails to predict the second homoclinic bifurcation for a positive α and the HL1 and HL2 models have pathological behavior at large Pe.

Previous studies of closure models, mostly focused on simple shear flows, emphasize the difference between the models. What is notable about the present results is the similarity among the model predictions for general two-dimensional homogeneous flows. All the closures predict the same regimes of director motion. The differences among them consist of shifts of the critical U, Pe and α values corresponding to transitions between director aligning, wagging and tumbling. In a nonhomogeneous flow, the LCP configuration depends not only on the local flow conditions but also on the history of deformation. If the variations in flow type and strain rate are large, the integrative effect along a streamline will obscure the differences between predictions of different closures. Hence, in such a flow, one may expect the LCP dynamics to be qualitatively the same for all the closures.

IV. NONHOMOGENEOUS FLOWS

In this section we apply the quadratic, the QuadR, the HL1Q and the Bingham closure models to a complex flow calculation. The HL1 and HL2 closures are not used because

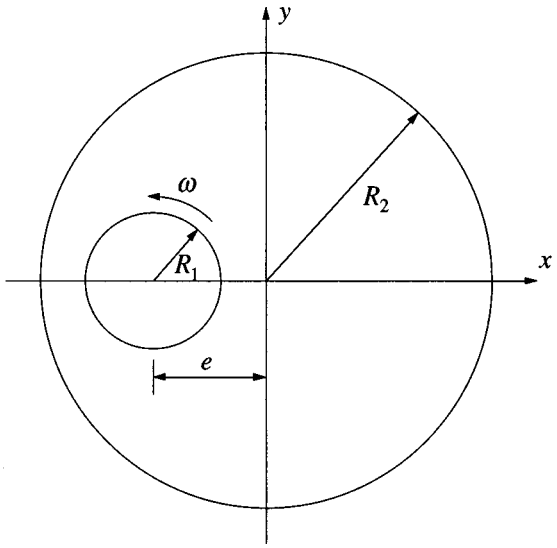

FIG. 9. The eccentric cylinder flow cell.

their solution diagrams differ greatly from that of the exact solution, and so they have little chance of outperforming the other closure models.

We choose the flow in an eccentric cylinder device as a test for the same reason that it was used in our previous study [Feng and Leal (1997)]. The geometry leads to a complex flow field with shear, extensional and rotational flow types in different regions of the domain. This offers a good opportunity for examining the effects of deformation history on the LCP behavior. Figure 9 shows the geometry of the eccentric-cylinder flow cell. The outer cylinder is stationary and the inner one starts abruptly at $t = 0$ with an angular velocity ω. We take $\Lambda = R_1/3$ as the characteristic length of the problem. Then $R_1 = 3$, $R_2 = 10$ and the distance between the centers of the cylinders is $e = 5$. The inertia of the fluid is neglected and the flow is governed by

$$\nabla \cdot \mathbf{v} = 0, \tag{16}$$

$$\mathrm{Re}\frac{\partial \mathbf{v}}{\partial t} = -\nabla p + \nabla^2 \mathbf{v} + \frac{c}{\mathrm{Pe}}\nabla \cdot \boldsymbol{\tau}, \tag{17}$$

where the Reynolds number is defined as $\mathrm{Re} = \rho\omega\Lambda^2/\eta_s$, with ρ and η_s being the density of the fluid and the constant solvent viscosity, respectively. The concentration parameter c is defined by

$$c = \frac{\nu kT}{2\eta_s D_r}. \tag{18}$$

The polymer stress tensor $\boldsymbol{\tau}$ is computed from Eq. (2) and influences the flow through Eq. (17). The fluid flow in turn affects the evolution of $\mathbf{A}$ through Eq. (1) [or Eq. (6) for the QuadR model]. The coupled system is solved by a finite element method. The flow is two dimensional and the LCP orientation distribution is assumed to be symmetric about the flow plane. This precludes the kayaking motion of the director that has been observed over a narrow range of parameters in simple shear. More details of the setup of the

problem and the numerics can be found in Feng and Leal (1997). We will only use in-plane initial orientations, although the log-rolling state may arise spontaneously at certain locations.

The following parameter values are used: $\beta = 1000$, $\mathrm{Re} = 1.11\times10^{-4}$, $(\nu L^3)^2 = 2\times10^6$, $c = 10$, $U = 6$ and $\mathrm{Pe} = 10$. The small Reynolds number ensures a short initial transient of the fluid flow after the startup. The crowdedness factor is typical of lyotropic systems used in experiments. It is not clear what c values are representative of real LCPs. Doraiswamy and Metzner (1986) and Mori *et al.* (1995) effectively estimated c by fitting the Doi theory with quadratic closure to steady shear viscosity measured for LCP solutions. This procedure is problematic. The model produces a steady-state shear viscosity because the quadratic closure artificially suppresses director tumbling. In the experiment, however, the steady state is a manifestation of the polydomain structure with each domain tumbling continuously. Here we choose a fairly small c so as to limit the effects of polymer stress on the flow field. This avoids the complication of severe flow modification and allows us to concentrate on the dynamics of the LCP, which serves as a test for the closure models. Generally one would expect the performance of the closures to vary depending on the values of U and Pe. It is not obvious what values are most suitable for our purpose. As will be seen presently, the quadratic model predicts similar features here as it does for $U = 20$ and $\mathrm{Pe} = 100$ in a previous study [Feng and Leal (1997)]. Therefore, we may hope for a certain degree of generality of the results obtained using the values of U and Pe listed above.

The flow kinematics in the eccentric cylinder geometry has been reported in Fig. 3 of Feng and Leal (1997). There is a recirculation eddy in the wide gap where the flow is rotational. There are two arclike regions above and below the inner cylinder that contain extensional flows, associated with the diverging and converging streamlines. The rest of the domain contains largely near-shear flows. Next, the predictions of the quadratic, QuadR, HL1Q and Bingham closure models will be described and compared.

A. The quadratic closure

The LCP dynamics for the quadratic closure is similar to that depicted in Fig. 9 of Feng and Leal (1997) at $U = 20$, $\mathrm{Pe} = 100$. The main features of the solution can be summarized as follows. The rotational flow in the recirculating eddy induces director tumbling. As a result, a tumbling domain appears periodically which is surrounded by a belt in which the director wags. Further out the director is steadily aligned with the flow. On the boundary of the domain, the director field is severely distorted and a pair of $\pm1/2$ disclinations form and travel along the boundary. When the director rotation inside the domain reaches multiples of 180°, the boundary disappears, and the domain will emerge and grow anew with the next cycle of director tumbling. Figure 10 shows the tumbling domain in its maximum size.

B. The QuadR closure

With the finite molecular aspect ratio in the QuadR model, the director behaves as if it were governed by the original Doi theory with the quadratic closure in a somewhat more rotational flow. Hence one expects a greater tendency toward director tumbling and wagging. The cyclic variation of the director field is similar to that for the quadratic closure. However, there are two new features. First, the area surrounding the inner cylinder now sees director wagging instead of steady alignment. Second, there appear two areas to the upper right and lower left of the inner cylinder in which the order parameter S is reduced [Fig. 11(a)]. This is probably a result of the decelerating flow in these areas

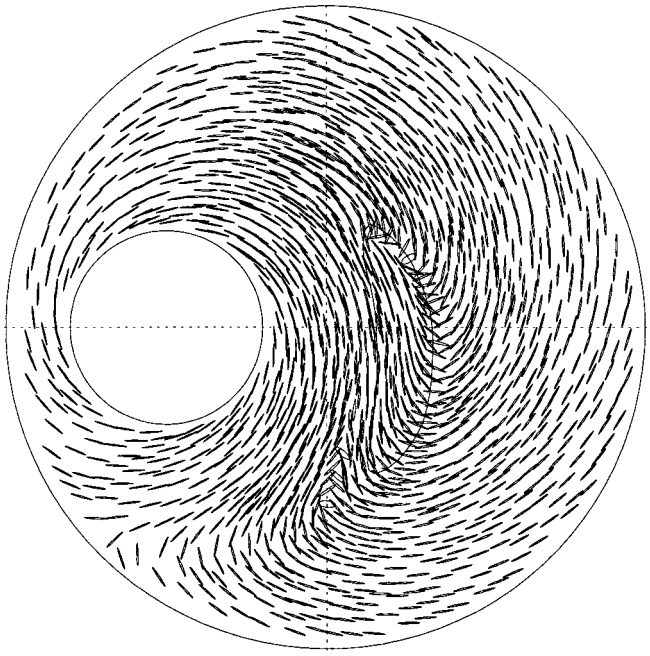

FIG. 10. A snapshot of the director field as predicted by the quadratic closure. $t = 79$. The loop delineates the tumbling domain in its maximum size.

related to the diverging streamlines. It is not clear why the pattern is absent or at least less conspicuous in Fig. 10 for the quadratic closure.

Each cycle of director tumbling is initiated at the right edge of area A. The tumbling propagates to the right and joins the tumbling that has emerged from the center of the recirculating eddy. This results in a much larger tumbling zone than that in Fig. 10. A pair of $\pm 1/2$ disclinations form on the boundary and travel downward as the tumbling domain grows towards the end of the cycle [Fig. 11(b)]. On the outer cylinder, the flow is simple shear and director tumbling is expected. But the local strain rate is about 30 times smaller than that at the inner cylinder and hence the tumbling period is extremely long.

C. The HL1Q closure

The initial development of the director field is similar to those of the quadratic and QuadR closures. The director wags in the area surrounding the inner cylinder with a greater amplitude than for the QuadR closure. Above the inner cylinder, director tumbling occurs in an arc-shaped strip [area A in Fig. 12(a)], which propagates to the right and later connects with the tumbling zone in the center of the eddy. The tumbling domain grows in time and its boundaries heal in much the same manner as for the QuadR model. Figure 12(b) shows the domain in its maximum size. Director tumbling also occurs in area B below the inner cylinder, creating a localized defectlike structure which heals periodically. Apparently, areas A and B correspond to the two low S regions for the QuadR closure in Fig. 11, only here the director tumbles in both areas instead of wagging. The tumbling domain is much wider thanks to the location of area A. The tumbling of the director in area A, area B and the center of the recirculating eddy occurs at different phase and period, giving the entire director field a quasiperiodic quality.

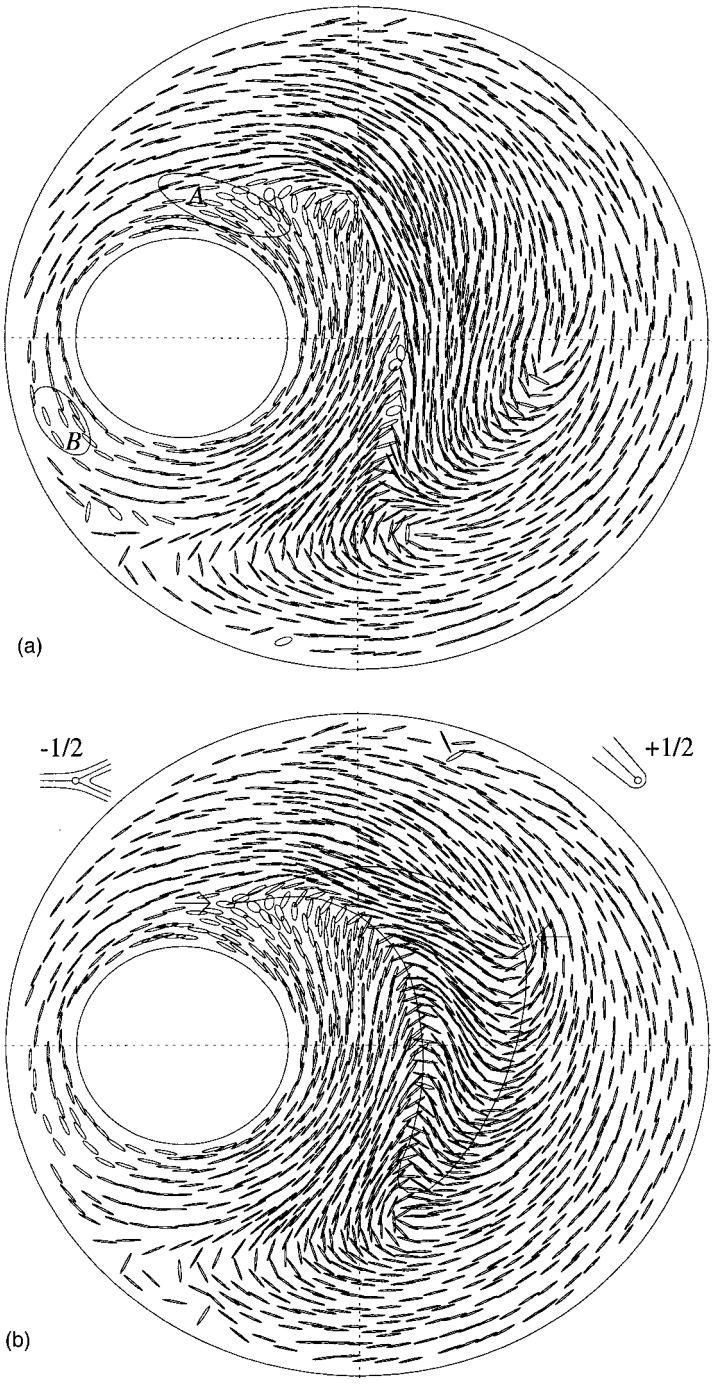

FIG. 11. The evolution of the director field as predicted by the QuadR closure. (a) $t = 80$. The lower order parameter in areas A and B is indicated by plumper ellipses; (b) $t = 112$. The loop delineates the tumbling domain. On its boundary there are a pair of $\pm 1/2$ disclinations indicated by the arrows and illustrated by the sketches.

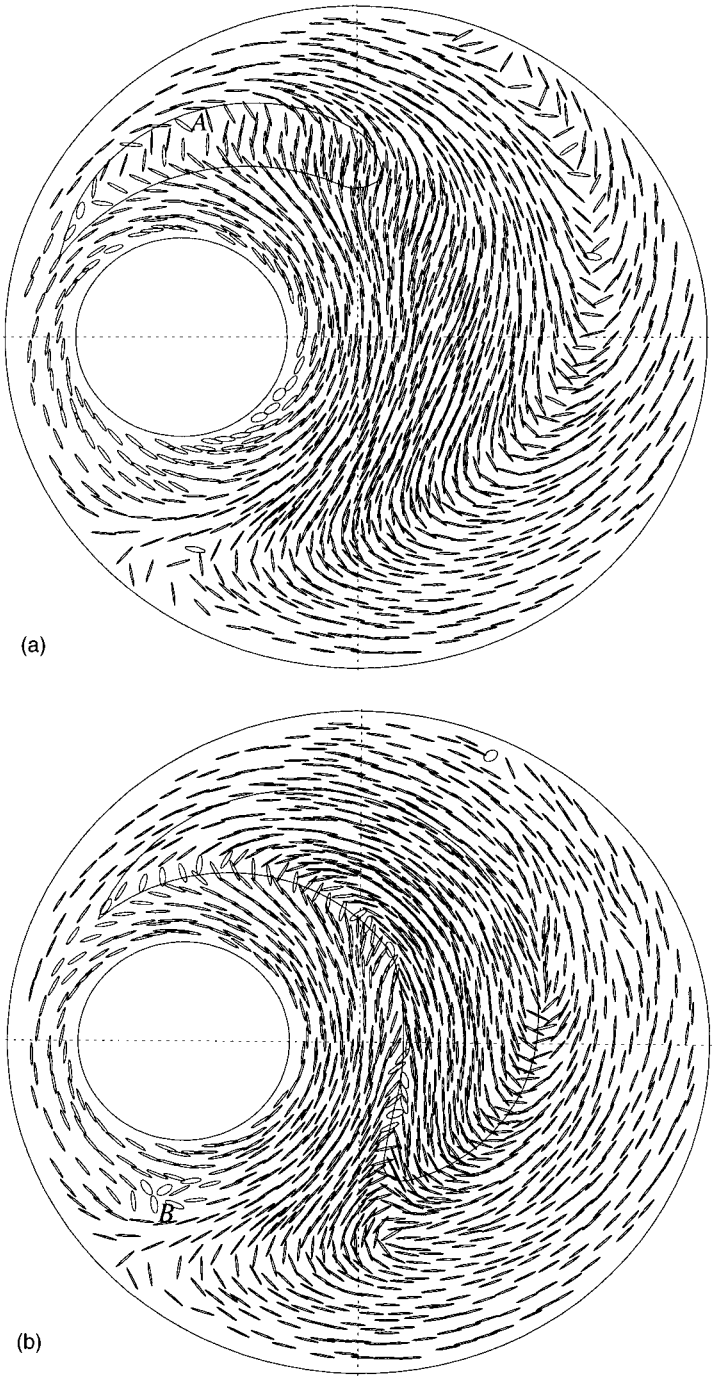

FIG. 12. The evolution of the director field as predicted by the HL1Q closure. (a) $t = 36$. Director tumbling starts in area A; (b) $t = 72$. The loop delineates the tumbling zone. Director tumbling also occurs in area B.

D. The Bingham closure

As for the QuadR model, the initial development of the director field leads to two low S regions [A and B in Fig. 13(a)]. Their positions are roughly the same as for the QuadR closure but the order parameter is even lower. Director tumbling originates from the right edge of area A, and propagates to the right to join the tumbling zone centered inside the eddy. The size of the tumbling domain, nearly fully grown in Fig. 13(b), is between those of the quadratic and QuadR closures.

One may also note that the ellipses in Fig. 13 are generally plumper than in the preceding figures; the Bingham closure predicts lower molecular order. This is not surprising since the quadratic closure overestimates the equilibrium order parameter S_{eq} [see Fig. 2 of Chaubal *et al.* (1995)], and the QuadR and HL1Q models have the same S_{eq}.

E. Comparison and discussion

As expected at the end of Sec. III, the *qualitative* nature of the inhomogeneous solution is indeed the same for all closures tested. In homogeneous flows, the difference between the closure models and the exact Doi theory is most prominent in the neighborhood of simple shear. In the nonhomogeneous flow computed, the deformation history includes greatly varying conditions far from shear and hence the predictions do not differ as much among models. In particular, the distinct inability of the quadratic model to predict tumbling in simple shear is hardly discernible in the simulation. The fact that the essential features of the solution are independent of the closure approximations is encouraging; these features are unlikely to be artifacts of the specific closure used, and we have probably captured the true LCP dynamics as predicted by the unapproximated Doi theory.

There are *quantitative* differences among the four simulations. The most obvious difference is in the size of the tumbling domain. The closure models are ordered as quadratic, Bingham, QuadR and HL1Q with increasing size of the tumbling zone. The models, in that order, also feature progressively more vigorous wagging and even tumbling in regions outside the recirculating eddy. One may see this ordering as one with an increasing proclivity toward periodic motions of the director. This is consistent with their respective behavior in homogeneous flows [see Fig. 7(b)]. For the quadratic closure, the tumbling domain originates and centers inside the recirculating eddy. For the other closures, there are two low S areas A and B close to the rotating cylinder, and the tumbling domain extends from the eddy to area A. Going to finer details of the four simulations, Fig. 14 compares the temporal variations of the order parameter and the orientation angle of the director at a fixed spatial point that is roughly at the center of the eddy. The quadratic closure has a longer period than the other three models. The Bingham closure stands out in that it predicts a lower order parameter, a fact already noted in Fig. 13. Since the Bingham closure gives the exact S_{eq}, the Bingham curves in Fig. 14 should be more accurate than the others.

V. CONCLUSION

In two-dimensional homogeneous flows, all six closure models considered in this article (quadratic, QuadR, HL1, HL1Q, HL2 and Bingham) predict three regimes of director motion: steady alignment, wagging and tumbling. HL2 stands out because it predicts spurious tumbling or large-amplitude wagging at high Pe in near-shear flows. The differences among the rest of the models consist of shifts of the critical U, Pe and α

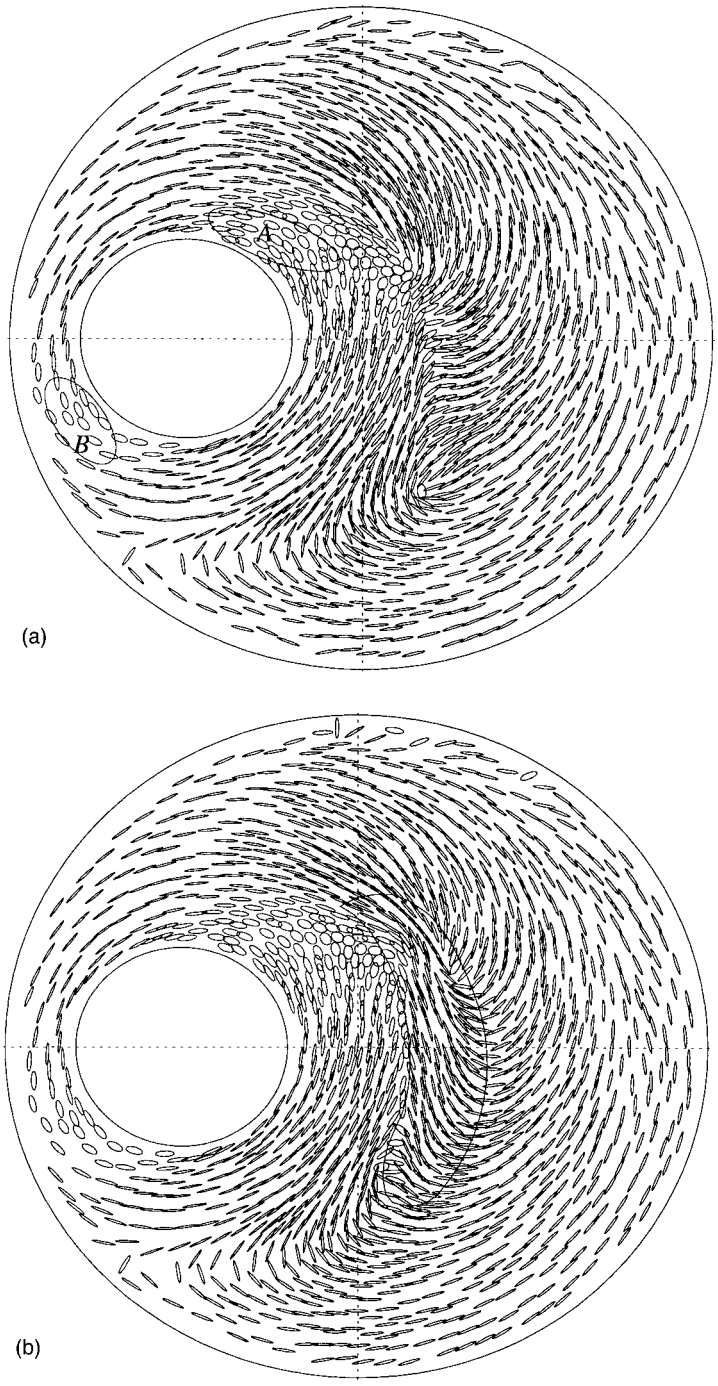

FIG. 13. The evolution of the director field as predicted by the Bingham closure. (a) $t = 20$. The molecular order is reduced in regions A and B; (b) $t = 108$. The loop delineates the tumbling domain.

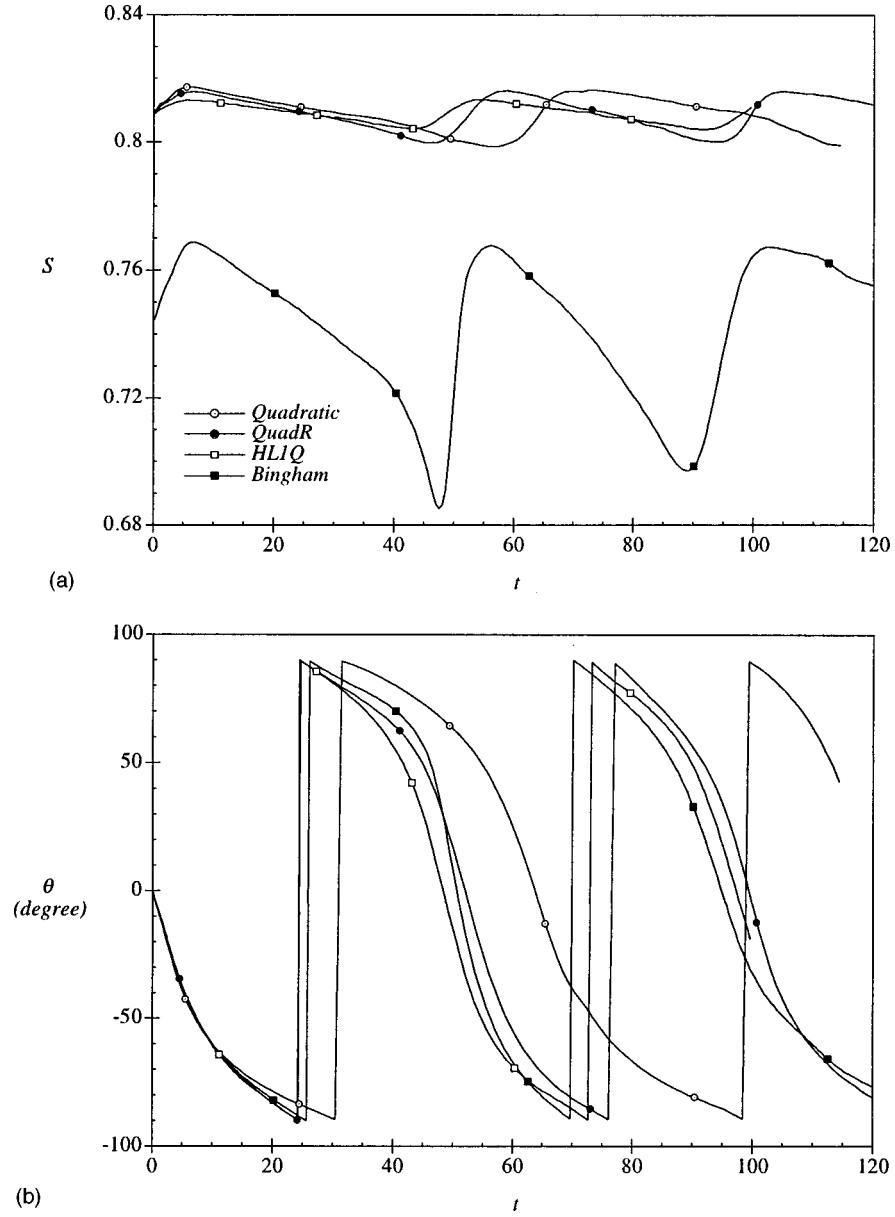

FIG. 14. Temporal variation of the LCP configuration at $(x,y) = (3,0)$ for different closure models. (a) The order parameter S; (b) the orientation angle of the director θ (same symbols as in a). At $U = 6$, the equilibrium order parameter $S_{eq} = 0.745$ for the Bingham closure and the unapproximated Doi theory and 0.809 for the other closures.

values for transitions between regimes. The Bingham closure gives the best approximation to the exact Doi theory. In particular, its prediction is exact in the weak flow limit.

In the inhomogeneous flow computed, the closure models predict the same essential features of the LCP behavior. This is expected to be true for most inhomogeneous flows containing regions of markedly different flow strength and flow types. (This excludes shear-dominated flows; for instance, the quadratic and Bingham closures will give dras-

tically different predictions in channel flows.) Without a solution of the exact Doi theory to compare with, it is not obvious which model performs best in simulating complex flows. A closer inspection of the order parameter at one fixed point suggests that the Bingham closure gives the most accurate prediction.

One may argue that the superiority of the Bingham closure in inhomogeneous flows has yet to be firmly established by comparing with the exact Doi theory. At present, however, we recommend the Bingham closure for use in simulating complex LCP flows. Its implementation is no more difficult than the other closure models. The QuadR and HL1Q closures give better predictions than the quadratic, HL1 and HL2 closures, but we see no circumstances that would favor them more than the Bingham closure.

ACKNOWLEDGMENTS

This research was supported by the Materials Research Laboratory at UCSB. The computation was done at the NSF Supercomputer Centers in San Diego and Pittsburgh.

References

Advani, S. G. and C. L. Tucker, ''Closure approximations for three-dimensional structure tensors,'' J. Rheol. **34**, 367–386 (1990).

Anczurowski, E. and S. G. Mason, ''Particle motions in sheared suspensions. XXIV. Rotation of rigid spheroids and cylinders,'' Trans. Soc. Rheol. **12**, 209–215 (1968).

Archer, L. A., and R. G. Larson, ''A molecular theory of flow alignment and tumbling in sheared nematic liquid crystals,'' J. Chem. Phys. **103**, 3108–3111 (1995).

Armstrong, R. C., R. Nayak, and R. A. Brown, ''The use of kinetic theory and microstructural models in the analysis of complex flows of viscoelastic liquids,'' Proceedings of the XIIth International Congress on Rheology, 1996, pp. 307–310.

Armstrong, R. C., S. Ramalingam, and D. E. Bornside, ''A finite-element model to predict structure development in spinneret flow of liquid-crystalline polymers,'' SPE ANTEC Proceedings, 1995, pp. 2590–2594.

Astarita, G., ''Objective and generally applicable criteria for flow classification,'' J. Non-Newtonian Fluid Mech. **6** 69–76 (1979).

Baek, S.-G., J. J. Magda, and R. G. Larson, ''Rheological differences among liquid-crystalline polymers. I. The first and second normal stress differences of PBG solutions,'' J. Rheol. **37**, 1201–1224 (1993).

Bhave, A. V., R. K. Menon, R. C. Armstrong, and R. A. Brown, ''A constitutive equation for liquid-crystalline polymer solutions,'' J. Rheol. **37**, 413–441 (1993).

Chaubal, C. V., Ph.D. thesis, University of California, Santa Barbara, 1997.

Chaubal, C. V. and L. G. Leal, ''A closure approximation for liquid crystalline polymer models based on parametric density estimation,'' J. Rheol. **42**, 177–201 (1998).

Chaubal, C. V., L. G. Leal, and G. H. Fredrickson, ''A comparison of closure approximations for the Doi theory of LCPs,'' J. Rheol. **39**, 73–103 (1995).

Chaubal, C. V., A. Srinivasan, Ö. Egecioglu, and L. G. Leal, ''Smoothed particle hydrodynamics technique for the solution of kinetic theory problems. Part 1. Method,'' J. Non-Newtonian Fluid Mech. **70**, 125–154 (1997).

Cintra, J. S. and C. L. Tucker, ''Orthotropic closure approximations for flow-induced fiber orientation,'' J. Rheol. **39**, 1095–1122 (1995).

Doi, M., ''Molecular dynamics and rheological properties of concentrated solutions of rodlike polymers in isotropic and liquid crystalline phases,'' J. Polym. Sci., Polym. Phys. Ed. **19**, 229–243 (1981).

Donald, A. M. and A. H. Windle, *Liquid Crystalline Polymers* (Cambridge University Press, Cambridge, 1992).

Doraiswamy, D. and A. B. Metzner, ''The rheology of polymeric liquid crystals,'' Rheol. Acta **25**, 580–587 (1986).

Feng, J. and L. G. Leal, ''Simulating complex flows of liquid crystalline polymers using the Doi theory,'' J. Rheol. **41**, 1317–1335 (1997).

Forest, M. G., Q. Wang, and S. E. Bechtel, ''One dimensional isothermal spinning models for liquid crystalline polymer fibers,'' J. Rheol. **41**, 821–850, (1997).

Hinch, E. J. and L. G. Leal, ''Constitutive equations in suspension mechanics. Part 2. Approximate forms for a suspension of rigid particles affected by Brownian rotations,'' J. Fluid Mech. **76**, 187–208 (1976).

Kuzuu, N. and M. Doi, ''Constitutive equation for nematic liquid crystals under weak velocity gradient derived from a molecular kinetic equation,'' J. Phys. Soc. Jpn. **52**, 3486–3494 (1983).

Kuzuu, N. and M. Doi, ''Constitutive equation for nematic liquid crystals under weak velocity gradient derived from a molecular kinetic equation. II. Leslie coefficients for rodlike polymers,'' J. Phys. Soc. Jpn. **53**, 1031–1040 (1984).

Larson, R. G., ''Arrested tumbling in shear flows of liquid crystalline polymers,'' Macromolecules **23**, 3983–3992 (1990).

Larson, R. G. and D. W. Mead, ''Toward a quantitative theory of the rheology of concentrated solutions of stiff polymers,'' J. Polym. Sci., Part B: Polym. Phys. **29**, 1271–1285 (1991).

Larson, R. G. and H. C. Öttinger, ''Effect of molecular elasticity on out-of-plane orientation in shearing flows of liquid crystalline polymers,'' Macromolecules **24**, 6270–6282 (1991).

Maffettone, P. L. and S. Crescitelli, ''The rigid rod model for nematic polymers: testing closure approximations with bifurcation analysis,'' J. Rheol. **38**, 1559–1570 (1994).

Marrucci, G. and F. Greco, ''A molecular approach to the polydomain structure of LCPs in weak shear flows,'' J. Non-Newtonian Fluid Mech. **44**, 1–13 (1992).

Marrucci, G. and P. L. Maffettone, ''Description of the liquid-crystalline phase of rodlike polymers at high shear rates,'' Macromolecules **22**, 4076–4082 (1989).

Mori, N., Y. Hamaguchi, and K. Nakamura, ''Numerical simulation of the spinning flow of liquid crystalline polymers,'' J. Rheol. **41**, 1095–1104 (1997).

Mori, N., Y. Tsuji, K. Nakamura, and C. Yoshikawa, ''Numerical simulations of the flow of liquid crystalline polymers between parallel plates containing a cylinder,'' J. Non-Newtonian Fluid Mech. **56**, 85–97 (1995).

Nayak, R., R. C. Armstrong, and R. A. Brown, ''Wavelet-FEM simulations of complex flows of rigid rods,'' Soc. Rheol. 68th Ann. Meeting, Galveston, Texas, Feb. 16–20, 1997.

Ramalingam, S. and R. C. Armstrong, ''Analysis of isothermal spinning of liquid-crystalline polymers,'' J. Rheol. **37**, 1141–1169 (1993).

Szeri, A. J. and D. J. Lin, ''A deformation tensor model of Brownian suspensions of orientable particles-the nonlinear dynamics of closure models,'' J. Non-Newtonian Fluid Mech. **64**, 43–69 (1996).

Szeri, A. J., S. Wiggins, and L. G. Leal, ''On the dynamics of suspended microstructure in unsteady, spatially inhomogeneous two-dimensional fluid flows,'' J. Fluid Mech. **228**, 207–241 (1991).

Walker, L. and N. Wagner, ''Rheology of region I flow in a lyotropic polymer: The effects of defect texture,'' J. Rheol. **38**, 1525–1547 (1994).

Wang, Q., ''Comparative studies on closure approximations in flows of liquid crystal polymers. I. Elongational flows. II. Fiber flows,'' J. Non-Newtonian Fluid Mech. **72**, 142–185 (1997).

Wang, H., R. C. Armstrong, and R. A. Brown, ''A finite-element model to predict structure development in extrusion of liquid-crystalline polymers,'' Proceedings of the XIIth International Congress on Rheology, 1996, pp. 167–168.